Supplement

Supplemental Methods

Dose finding

Supplemental Figure 1

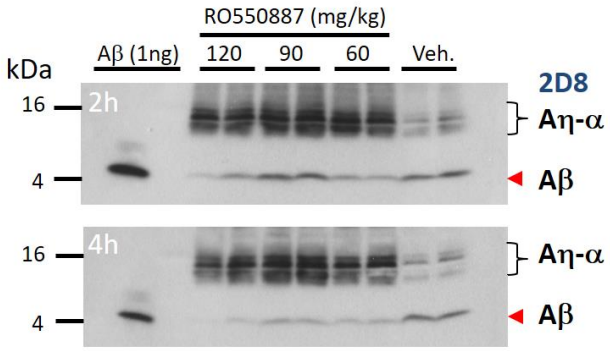

Supplemental Figure S1: Dose finding analysis. BACE1 inhibition caused reduced levels of soluble Aβ and an increase of Aη-α in brains of the TG-BSI mice compared to TG-VEH controls 4 hours after treatment already at a dose of 60 mg/kg.

Aβ-PET

Mice were anesthetized with isoflurane (1.5%, delivered at 3.5 L/min) and received an injection of 10.6 ± 2.4 MBq [^{18}F]-florbetaben to a tail vein. After placement in the aperture of the Inveon DPET (Preclinical Solutions, Siemens Healthcare Molecular Imaging), a single frame emission recording was obtained in the interval 30-60 min p.i., followed by a 15-min transmission scan using a rotating [^{57}Co] point source. The image reconstruction procedure consisted of a 3D ordered subset expectation maximization (OSEM, 4 iterations) and a 3D maximum a posteriori (MAP, 32 iterations) at a zoom factor of 1.0, and with scatter, attenuation, and decay corrections, resulting in a final voxel dimension of 0.78 x 0.78 x 0.8 mm. The origin of the Aβ-PET images was concealed from the operator for further analyses.

Static 30-60 min datasets were co-registered to an MRI mouse atlas (Dorr, Sled et al. 2007) by a manual rigid-body transformation (TX_{rigid}) using the PMOD fusion tool (V3.5, PMOD Technologies Ltd.). Templates were generated by averaging all age

specific PET scans of TG and WT groups. In the second step, a reader-independent fine co-registration to specific templates was performed (Overhoff, Brendel et al. 2016). Here, the initial manual µPET-to-MRI atlas fusion images were normalized by non-linear brain normalization (TX_{BN}) to the age-specific templates using the PMOD brain normalization tool (equal modality; smoothing by 0.6 mm; nonlinear warping; 16 iterations; frequency cutoff 3; regularization 1.0; no thresholding). The concatenation of TX_{rigid} and TX_{BN} was then applied to µPET frames in the native space, so as to obtain optimal resampling with a minimum of interpolation. For VOI-based analyses, a hindbrain white matter VOI comprising 67 mm^3 served for normalization and two bilateral frontal cortex VOIs comprising 12 mm^3 each, were employed for calculation of Aβ-PET cortex-to-cerebellum standardized-uptake-value-ratios ($SUVR_{CTX/CBL}$), as described earlier (Overhoff, Brendel et al. 2016).

Histochemical analyses

Cerebral hemispheres randomly selected for histochemistry were fixed by immersion in 4% paraformaldehyde at 4 °C for two days. A mean of five representative 50 µm thick slices per animal were then cut in the sagittal plane about 1.5 mm from the midline using a vibratome (VT 1000 S, Leica, Wetzlar, Germany). The slices were permeabilized overnight in 2% Triton X-100 in phosphate buffered saline (PBS; pH 7.4) at room temperature. The unbound dye was removed by three washing steps with PBS, and the slices were then mounted on microscope slides with fluorescent mounting medium (Dako, Germany). 3D image stacks for each hemisphere were acquired on an anepi-fluorescence microscope (Axio Imager.M2 with ApoTome.2, Jena, Zeiss, Germany). Imaging of the whole slice was performed in tile scan mode, which allows automatic stitching of an array of fields of view. For this imaging, the methoxy-X04 was excited at 405 nm, and the emitted light was collected from 410 to

585 nm. The area and number of plaques were automatically counted using Imaris software (Imaris 7. 6.5; Bitplane, Zurich) in a region (0.27 ± 0.04 mm³) defined to match the frontal cortex VOI as applied for Aβ-PET image analysis.

Supplemental Results

Supplemental Figure S2

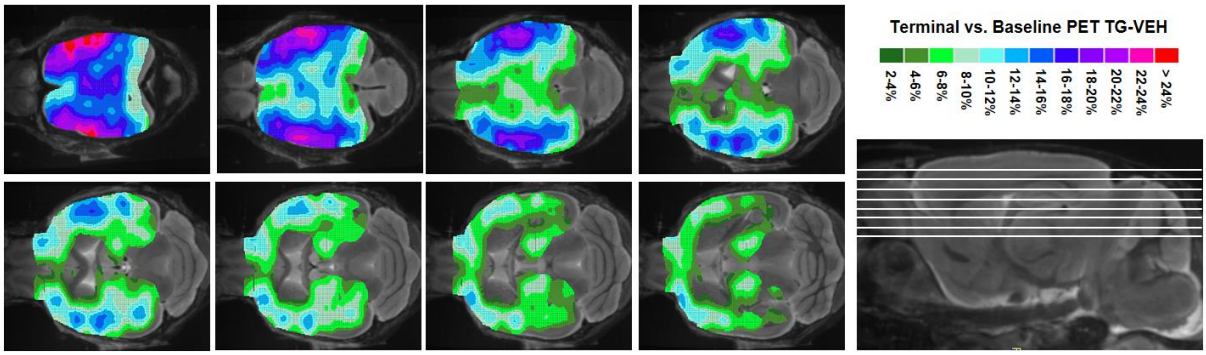

Supplemental Figure S2: Isobaric lines (2% steps) depict amyloid progression in TG-VEH mice between baseline and terminal PET scans. Axial slices through the cranial half of the mouse brain are illustrated upon a T1w MRI template.

Supplemental Figure S3

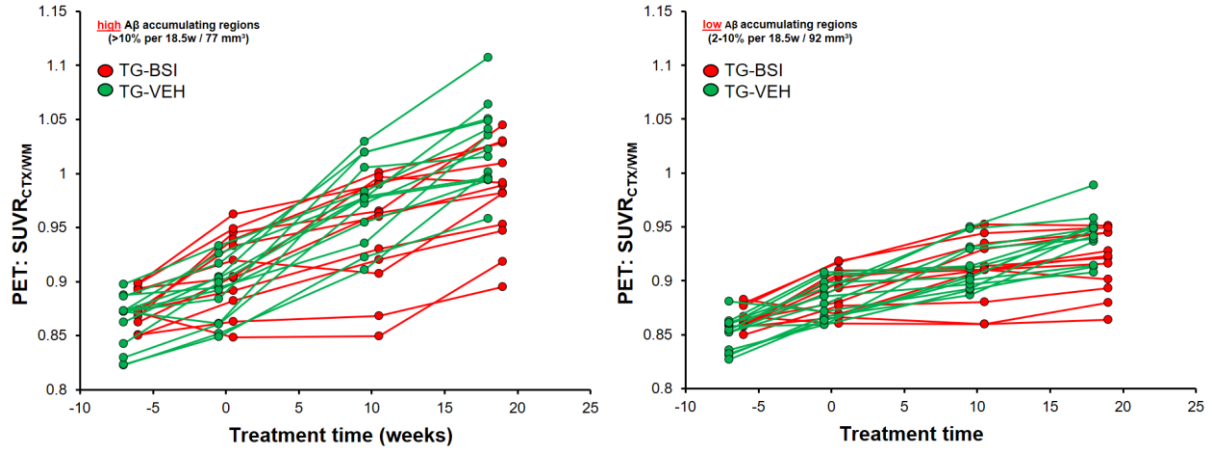

Supplemental Figure S3: Individual longitudinal Aβ-PET imaging of BACE1 inhibition versus vehicle in high (**A**) and low (**B**) Aβ accumulating brain regions.

Supplemental References:

Dorr, A., J. G. Sled and N. Kabani (2007). "Three-dimensional cerebral vasculature of the CBA mouse brain: a magnetic resonance imaging and micro computed tomography study." Neuroimage **35**(4): 1409-1423.

Overhoff, F., M. Brendel, A. Jaworska, V. Korzhova, A. Delker, F. Probst, C. Focke, F. J. Gildehaus, J. Carlsen, K. Baumann, C. Haass, P. Bartenstein, J. Herms and A. Rominger (2016). "Automated Spatial Brain Normalization and Hindbrain White Matter Reference Tissue Give Improved [(18)F]-Florbetaben PET Quantitation in Alzheimer's Model Mice." Front Neurosci **10**: 45.